ADVANCED MATERIALS INTERFACES
Open Access
www.advmatinterfaces.de



# Mechanical Deformation Effects on Flexible Thin Film Transistors: A Comparison Between 6,13-Bis(Triisopropylsilylethynyl)Pentacene and N,N′-Bis-(2-Ethylhexyl)-1,7-Dicyanoperylene-3,4:9,10-bis(Dicarboximide) Derivatives

*A. Mascia,* M. Concas, E. Podda, G. Casula, S. Lai, and P. Cosseddu**

**In this work, the investigation of the surface strain-induced electrical changes in two commonly employed solution-processable organic semiconductors, i.e., 6,13-bis(triisopropylsilylethynyl)pentacene (TIPS-Pentacene) and N,N′-bis-(2-ethylhexyl)−1,7-dicyanoperylene-3,4:9,10-bis(dicarboximide) (N1400), is reported. A detailed electromechanical characterization of two sets of flexible organic field-effect transistors is performed, clearly demonstrating that both systems are affected by mechanical deformation in terms of electrical performance. However, the N1400 system shows a much more stable and reproducible response, even after continuous mechanical stress. XRD and AFM analysis demonstrate that such difference is mainly related to the changes induced on the two thin film morphology by the applied deformations.**

## 1. Introduction

Organic conjugated molecules have gained considerable attention in the past decades, allowing for the fabrication of low-cost and light weighted devices on flexible plastic substrates, and usually with cost-efficient technologies, opening an entirely new market segment.[1–5] Organic field-effect transistors (OFETs) are recognized as key tools/building blocks for the implementation of electronic logic circuits[6,7] and have been intensively studied and employed for many applications, such as displays, smart tags, and sensors.[8–12] Aside from the cost efficiency of the fabrication procedures, flexibility represents one of the main advantages of this new technology. In fact, the possibility of adapting the fabricated devices on different kinds of deformable, flexible, and stretchable substrates, is a peculiar characteristic of such organic materials that pave the way for various application scenarios. However, for the fabrication of flexible electronic systems, it is mandatory that all devices must be able to withstand mechanical deformations without experiencing a degradation/variation of their electronic properties. Therefore, the effect of mechanical deformation on the device's characteristics is a highly discussed topic. For these reasons, several studies have been performed over the past years in order to better understand the electromechanical behavior of flexible electronic devices.[13–17]

As a matter of fact, it has been found that the performances of organic semiconductor-based devices are generally severely affected by mechanical deformation,[18–22] however, the effect of mechanical deformation on the electrical behavior of organic semiconductor-based devices can be dominated by many different details. The intrinsic properties of the employed semiconductor, the morphological properties of the deposited films, and also the overall structure and geometry of the fabricated devices. In particular, the surface strain induced on the active layer usually gives rise to deformation in the morphology of the deposited active layer. As hopping transport in such systems is strongly related to the morphological features, this effect is generally translated into a pronounced variation in hopping transport and mobility, leading to influence the output current of the devices. Such dependence strongly varies for different organic semiconductor small molecules. In general when long polymeric molecules are used, which generally give rise to very small crystal domains in the active layer,[22,23] this effect is less pronounced. When systems based on larger crystallites are employed, generally based on small molecules, the effect is much more evident. However,

A. Mascia, M. Concas, G. Casula, S. Lai, P. Cosseddu
Department of Electrical and Electronic Engineering
University of Cagliari
via Marengo 3, Cagliari 09123, Italy
E-mail: antonello.mascia@unica.it; piero.cosseddu@unica.it
E. Podda
Centre for Research University Services – CeSAR
University of Cagliari
Cittadella Universitaria di Monserrato
Monserrato (Cagliari) 09042, Italy

The ORCID identification number(s) for the author(s) of this article can be found under https://doi.org/10.1002/admi.202400783



**DOI: 10.1002/admi.202400783**

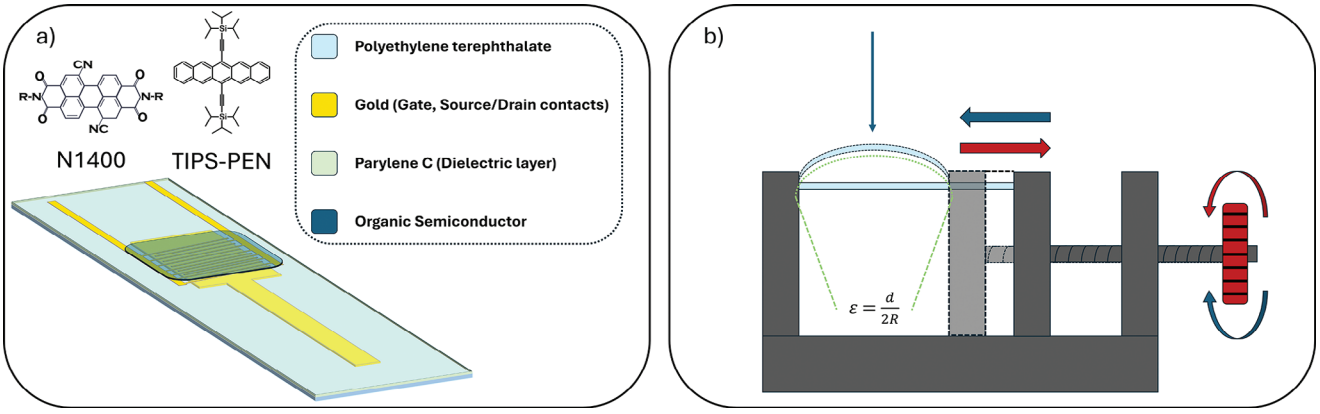


**Figure 1.** Schematic representation of the a) OFET with the employed materials and b) of the experimental set up employed for the electromechanical characterization.

it was also demonstrated that even by using the same small molecules, and properly tuning the initial morphological properties (i.e., average grain dimensions), it is possible to modulate the response of such devices to deformation, a clear indication that the morphology plays a fundaments role in this process.

More than this, it was also found that sensitivity to surface strain is typically reproducible and recoverable over a certain range of mechanical deformation,[23] this feature was exploited in the fabrication of OFET-based mechanical sensors.[24–26] However, in most cases, when deformations exceed 1–1.5% of surface strain, depending on the employed device structure, and semiconductor molecule, an irreversible behavior regime is reached, meaning that these devices cannot be employed in applications that foreseen deformations larger than such critical value.

On the other hand, there are also many applications where such mechanical sensitivity is undesirable because the devices have to be unaffected by applied stimuli and therefore operate normally even during mechanical deformation. For all these reasons, the study of the mechanical properties of organic semiconductors is of crucial importance to satisfy the different requirements of these applications.

In this paper, the effect of mechanical deformation in the performances of OFETs based on two different small molecules, namely 6,13-bis(triisopropylsilylethynyl)pentacene (TIPS pentacene, from now on TIPS-PEN) and N,N′-bis-(2-ethylhexyl)−1,7-dicyanoperylene-3,4:9,10-bis(dicarboximide) derivative (N1400), is discussed.

In fact, TIPS-PEN is a widely employed semiconductor, generally chosen because it can be very easily processed from solution by using drop-casting process. N1400 represents one of the few solution-processable n-type organic molecules with demonstrated high stability in air. This point makes such molecular system very interesting for the development of low-cost, long lasting flexible electronic systems, even if such molecule is generally characterized by a smaller mobility. In this study, a thorough electromechanical characterization is presented, showing the effect of mechanical deformation on the most representative electrical parameters, such as charge carrier mobility and threshold voltage. Moreover, we have also performed fatigue tests on both systems that gave rise to a very interesting different behavior. The results will be discussed on the basis of morphological and structural characteristics derived by atomic force microscopy (AFM) and X-ray diffraction (XRD).

## 2. Experimental Section

All the measured devices were fabricated using a bottom gate bottom contact structure reported in **Figure 1a**. Starting from a flexible polyethylene terephthalate (PET, thickness d = 175 μm) a gold gate electrode was realized by means of thermal evaporation through a shadow mask. After that, a 1.5 μm thick Parylene C (Specialty Coating Systems) film, which will act as the gate dielectric, was deposited by Chemical Vapor Deposition (CVD). A gold source and drain electrodes were fabricated by thermal evaporation and patterned by a standard photolithographic process, using an interdigitated structure (W/L = 1200). As organic semiconductors (OSCs) the 6,13-bis(triisopropylsilylethynyl)pentacene (TIPS-PEN) and the N,N′-bis-(2-ethylhexyl)−1,7-dicyanoperylene-3,4:9,10-bis(dicarboximide) derivative (N1400) were employed. In particular, for preparing the TIPS-PEN based devices a 0.5 wt.% solution using toluene was employed, while a 1 wt.% solution in 1,2 dichlorobenzene was used for the N1400-based transistors. All the devices were fabricated in ambient conditions. TIPS-PEN was deposited by drop casting the solution directly on the interdigitated structure, keeping the substrate at a constant temperature of 80 °C during the deposition, while N1400 was deposited by spin coating (60 ss at 1500 rpm). For both an annealing step (30 min at 80 °C) was carried out after the deposition.

Both electrical and electromechanical characterization were carried out at room temperature in ambient conditions using an Agilent HP 4155 Semiconductor Parameter Analyzer, provided with gold tips for contacting the electrodes. For electromechanical characterization, the connection of the device was realized by gluing a thin copper wire, with an average diameter ≈150 μm, onto the transistor terminals by using a silver paste. It is important to underline that, in order to be sure that this part of the device does not influence the electrical behavior of the devices during deformation, wires have been glued in an area that is not going to be deformed during the electromechanical tests.

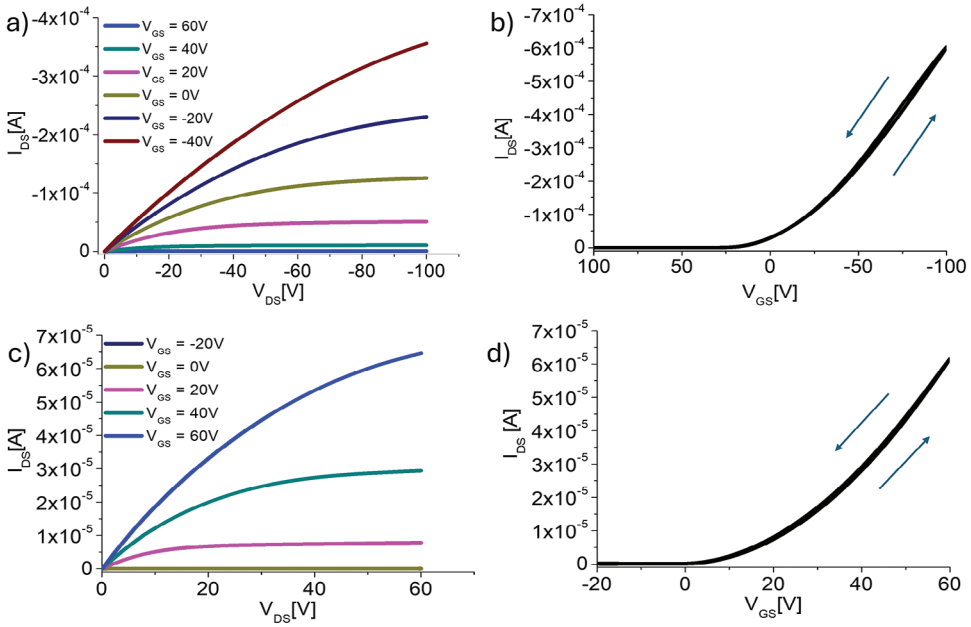


**Figure 2.** Output and Transfer characteristics obtained from a,b) TIPS-PEN, and c,d) N1400 based OFETs.

Figure 1b reports the experimental setup employed for the electro-mechanical characterization. The device was placed between two armatures, one of these two is fixed, whereas the second can be finely moved by means of an adjusting screw. The bending radius has been accurately estimated in order to obtain the corresponding surface strain value. Taking into account that, for uniaxial deformations and device thickness negligible with respect to the substrate thickness, the surface strain $\epsilon$ is defined as $\epsilon = \frac{d}{2R}$, where d is the substrate thickness and R is the bending radius. For all the characterized set of devices, the surface strain varied from 0.1% up to 4.5%.

## 3. Results and Discussion

### 3.1. OFETs Electrical Characterization

The typical output (a,c) and transfer (b,d) characteristic curves of the fabricated devices are reported in **Figure 2**. For all devices, both mobility and threshold voltage were derived from the transfer characteristics in the saturation regime; average values and 1-$\sigma$ tolerance bands for these parameters are reported in **Table 1**. Since the hysteresis was negligible for all devices, mobility and threshold voltage have the same value both in forward and backward gate voltage sweep.

**Table 1.** Comparison of the most meaningful electrical parameters for the two sets of OFETs, where N represents the number of devices that underwent a full electromechanical characterization.

| OSC | Mobility [$cm^2\ Vs^{-1}$] | $V_T$ [V] |
|---|---|---|
| TIPS-PEN (N = 5) | $7{\cdot}10^{-2} \pm 6{\cdot}10^{-2}$ | 38 ± 20 |
| N1400 (N = 5) | $3{\cdot}10^{-3} \pm 1{\cdot}10^{-3}$ | 3.4 ± 1.3 |

### 3.2. OFETs Electromechanical Characterization

The electromechanical testing procedure was performed as follows. At first, the device was characterized in flat conditions, afterward it was bent at a certain radius and the transfer curves were recorded during the mechanical deformation. At the end of this measurement, the device was placed back to the flat condition and its transfer curve was measured one more time. In this way, i) mechanical deformation-induced changes in figure of merit such as output current, mobility, and threshold voltage, and ii) reversibility of devices' electrical behavior after deformation were evaluated. The relative current and mobility variations are measured with respect to the transfer curve measured right before the considered deformation. Moreover, for each bending radius the measurement was repeated at least three time (always passing from the flat state), to make a statistical analysis. For both N1400 and TIPS-PEN, a set of five samples have been characterized, in order to evaluate the average behavior of different transistors. Representative examples of the behavior of TIPS-PEN and N1400-based devices is reported in terms of transfer characteristics curves in **Figure 3**. It is possible to notice that bending, inducing a surface strain on the device active layer, leads to a visible reduction of the transistor output current in both kinds of devices.

As previously introduced, similar behavior was already observed on different organic semiconductor-based transistors,[19,21,23] and more recently we have reported a detailed analysis of the influence of mechanical deformation on TIPS-PEN based devices,[27,28] which is taken as a benchmark for this work. The average results are presented in **Figure 4**, where the evolution of the most meaningful electrical parameters versus the applied surface strain is reported, i.e., relative output current variation, relative mobility variation, and threshold voltage variation. Sensitivity in terms of current variation is reported as $\Delta I_D/I_{D0} = (I_{bent}\text{-}I_0)/I_0$, being $I_{bent}$ and $I_0$ the current values

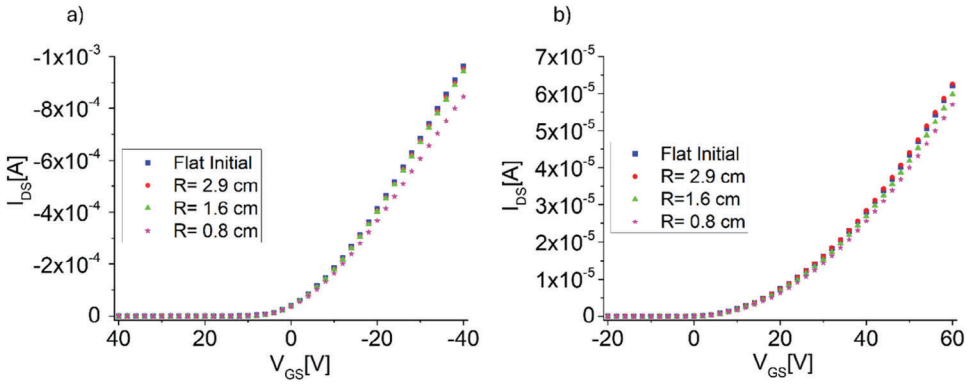


**Figure 3.** Transfer characteristics recorded before and during mechanical deformation at different bending radii on a) TIPS-PEN- and b) N1400- based OFETs.

recorded in the bent and flat state, respectively. Similarly, sensitivity calculated in terms of mobility is $\Delta\mu/\mu_0 = (\mu_{bent}-\mu_0)/\mu_0$, being $\mu_{bent}$ and $\mu_0$ mobility values in the bent and flat state respectively. As regards threshold voltage sensitivity, an absolute variation $\Delta V_{th} = V_{thbent}-V_{th0}$ is considered. In the latter, $V_{thbent}$ and $V_{th0}$ are threshold voltage values calculated in the bent and flat state, respectively.

It can be clearly observed that applying a surface strain induces a very reproducible effect in all the fabricated devices, as can be observed from the limited error bars reported in the graph. In all cases, a reduction of the output current was observed in both the investigated systems.

At this point several observations can be drawn. First of all, current reduction can be related to a corresponding mobility reduction observed in all the characterized devices. It can be also observed that in the two systems, the applied surface strain induces a small, but visible, variation (increase in its absolute value) of the transistor's threshold voltage. Both reported effects, concur

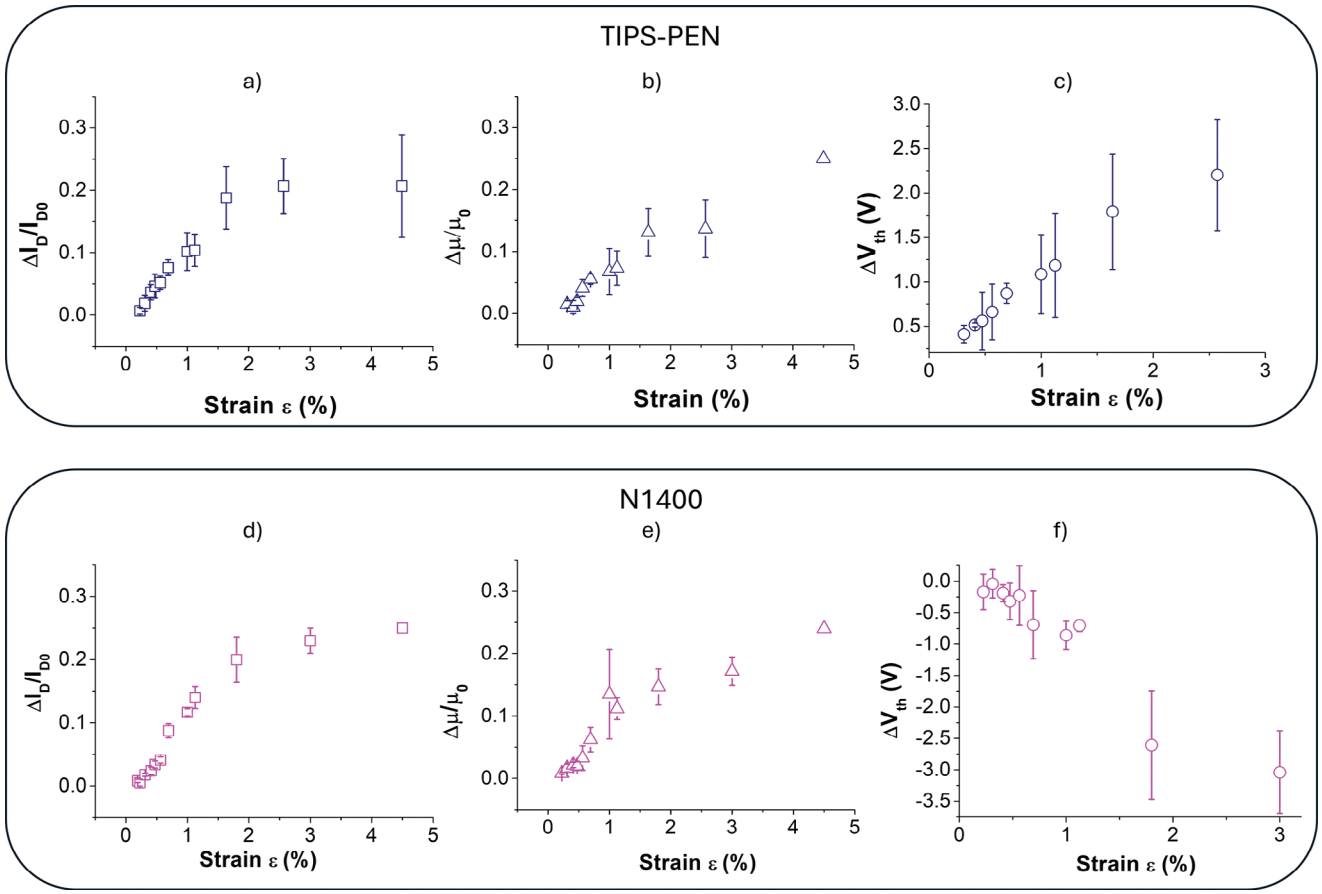


**Figure 4.** Relative variation of the output current and mobility and variation of the threshold voltage in a–c) TIPS-PEN and d–f) N1400 OFETs.

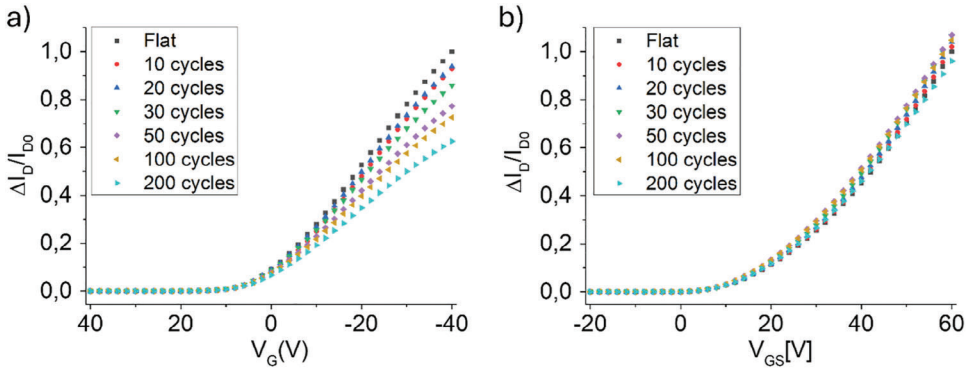


**Figure 5.** Fatigue tests performed on a) TIPS-PEN and b) N1400 based devices, by applying a deformation of 0.8% several times. It can be clearly noticed that TIPS-PEN based devices show a much more pronounced degradation upon cycling tests, even if performed under the defined critical strain value. On the contrary, N1400 devices show a much more pronounced stability.

in the overall decrease of the transistors output current during mechanical deformation.

Notably, when strain is kept below 1.5%, the device's behavior is fully reversible, and the device output current recovers to its initial state as soon as the deformation is removed. On the contrary, when deformations inducing strain values larger than 1.5% are applied, the device behavior is no longer reversible, indicating that the device structure is irreversibly damaged. In previous works, such effect has been reported to be dependent on cracks formation in the source and drain electrodes.[20] For such reasons, the following electrical characterization has been performed within the reversibility range and were aimed at evaluating the effects caused by fatigue on both types of devices. The fatigue tests consisted of bending cycles that were performed by measuring output current values first in flat conditions and subsequently by applying a surface strain of 0.8% for a certain number of times. After each bending cycle, a new transfer curve was measured in flat conditions and compared to the previous one.

As can be clearly observed from the plots reported in **Figure 5**, the two systems gave rise to a very different response to fatigue. Even if these experiments were performed within the reversibility range, TIPS-PEN based transistors are severely affected by such fatigue tests. It can be clearly observed that after 200 cycles the device's output current is reduced by almost 50%. This is correlated to a reduction of carrier mobility and an increase in the threshold voltage, which is permanent.

On the contrary, N1400 devices are characterized by a much better response, as the average current and mobility reduction after a prolongated cycling test is ≈10%.

### 3.3. XRD and AFM Analysis

In order to shed some light on the observed phenomenon, a structural and morphological investigation of the deformed thin films was carried out. XRD analyses were carried out on thin films of both N1400 and TIPS-PEN devices and are summarized in **Figure 6**a,b, respectively. The XRD pattern of the PET-based polymeric substrate in the angular range 3–35 °($2\theta$) strongly reflects its nature featuring four broad peaks at $2\theta$ = 13.8°, 15.6°, 23.8°, and 26.8°, respectively, with the latter being the most intense.

The presence of the crystalline organic semiconductor in N1400-based devices is reflected on the XRD patterns with an additional broad peak (Figure 6a) that corresponds to the (001) diffraction of the triclinic phase elucidated by means of ab-initio X-ray methods.[29] The XRD patterns collected on the same

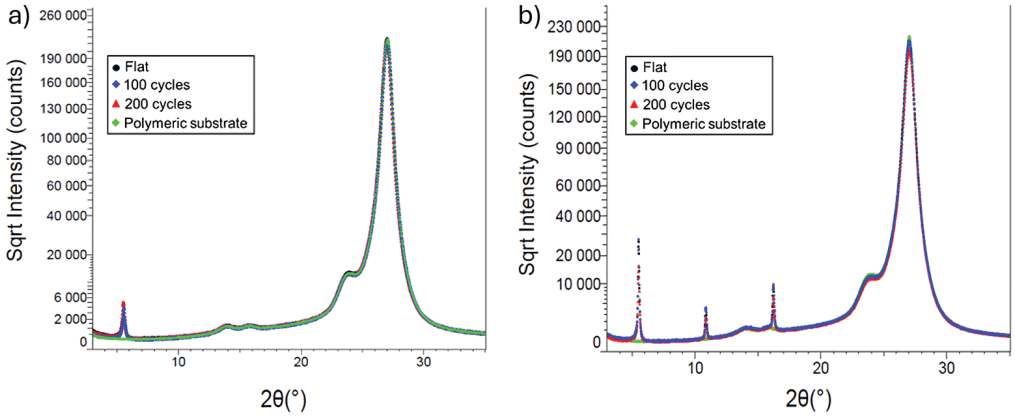


**Figure 6.** X-ray diffraction analyses on a) N1400 and b) TIPS-PEN devices before (black dots) and after 100 bending cycles at R = 1.6 cm (blue squares) and after additional 100 bending cycles at R = 0.8 cm (red triangles).

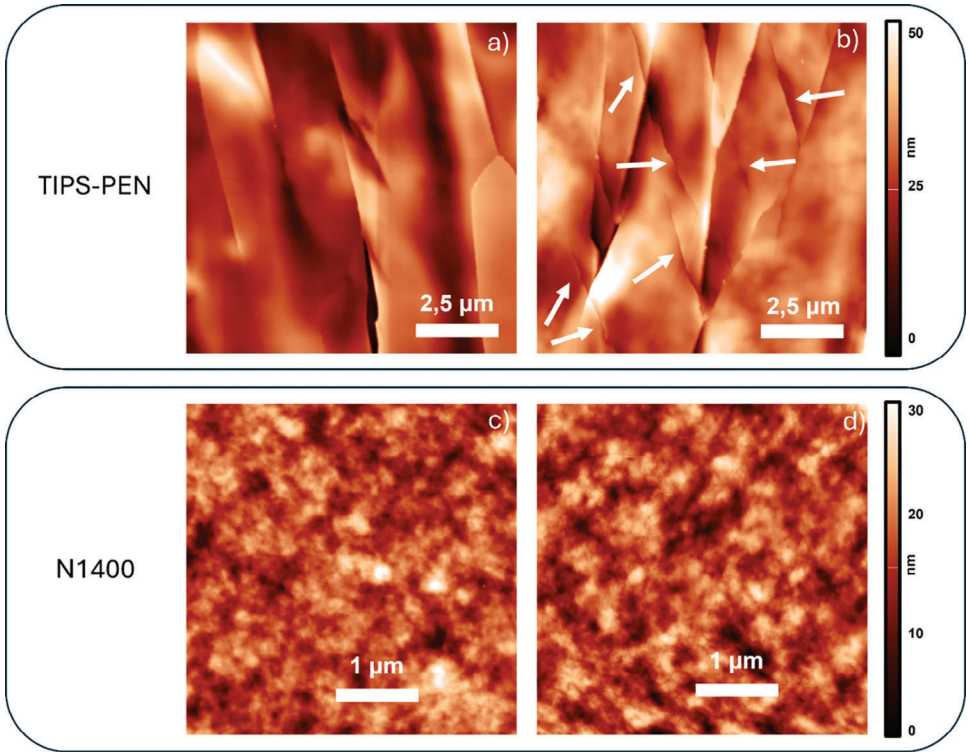


**Figure 7.** AFM images relative to TIPS-PEN film a) before bending and b) after bending, where cracks are clearly visible, and N1400 c) before bending and d) after bending where there is no evident crack in the structure.

device after 100 bending cycles at R = 1.6 cm and after additional 100 bending cycles at R = 0.8 cm (Figure 6a) showed negligible variations suggesting the preservation of its crystal structure. Similarly, the XRD analyses performed on TIPS-PEN devices (Figure 6b) before and after the bending cycles showed three sharp peaks at $2\theta = 5.3°$, 10.6°, and 16.0° in agreement with what was reported in the literature.[30,31] Peak profiles and intensities are barely affected by the bending cycles of thin films and clearly indicate that such deformations do not induce an irreversible change in the crystal structure of the deposited thin films.

To achieve a deeper understanding of the morphological features, AFM imaging was carried out, revealing a significant difference in the two deposited films, as shown in **Figure 7**. TIPS-PEN films, as previously reported in the literature,[27] are characterized by very large crystallites, whereas N1400 thin films are characterized by a much more pronounced polycrystalline structure, with crystallite dimensions generally ranging ≈200 nm.

When a severe deformation is applied to the two films, the effect on the morphology is significantly different. When a surface strain close to 1% is applied, cracks start to be formed in the TIPS-PEN crystallites, becoming much more pronounced for repeated deformations. This effect is clearly visible in Figure 7b, reporting the morphology of a TIPS-PEN thin film after 200 cycles of deformations at 0.8% of strain. We assume that such permanent degradation of the active layer morphology is responsible for the permanent changes in the electrical behavior observed in the reported samples. These findings seem to be in good agreement with what was already reported by Cramer et al.[27] On the contrary, N1400 thin film seems to give rise to a much more robust and elastic structure. In fact, no significant changes in the polycrystalline film can be observed. This effect can be clearly explained by considering the high concentration of grain boundaries present in the polycrystalline film, which are capable to accommodate such surface strain, giving the overall film a more elastic behavior, which was not observed in the TIPS-PEN films. Therefore, it is possible to conclude that such irreversible morphological damages in the latter system, even if they do not bring to a complete failure of the device, yet lead to a permanent decrease of their performances, which was not observed in the N1400 based OFETs, which are thus characterized by a much more robust morphology.

## 4. Conclusion

In this paper, the effect of mechanical deformation on two commonly employed organic semiconductor-based transistors was investigated. The obtained results demonstrate that device performances are affected by mechanical deformation due to a reduction of the carrier mobility and threshold voltage shift induced by the applied surface strain. This behavior was found to be linear and reproducible for deformations below 1%, indicating that such devices can potentially be employed for the fabrication of flexible strain sensors.

However, under continuous and cyclic deformation, even at low strain levels, the two systems give rise to markedly different mechanical behavior; particularly, TIPS-PEN-based OFETs show irreversible changes, whereas N1400-based devices maintain highly reproducible performance, making the latter a promising

candidate for long-lasting, flexible mechanical sensors and electronic circuits.

The correlation between structural, morphological, and electromechanical characterizations demonstrated that a continuous mechanical deformation does not alter the polycrystalline structure in either system. However, in TIPS-PEN-based devices, the deformation affects the morphology of the thin films, which likely contributes to the reduced reproducibility of their electrical behaviours. In contrast, the chemical structure of the N1400 offers greater stability under deformation, leading to more consistent performance.

## 5. Experimental Section

*Device Fabrication*: All the devices were fabricated on a polyethylene terephthalate (PET, thickness d = 175 µm, Goodfellow) substrate that was carefully cleaned by sonication in acetone, isopropanol, and deionized water. At first, a gold gate electrode was realized by means of thermal evaporation through a shadow mask. After that, as a gate dielectric layer, a 1.5 µm thick Parylene C (Specialty Coating Systems) film was deposited by chemical vapor deposition (CVD). Gold source and drain electrodes were patterned by a standard photolithographic process, using an interdigitated structure (W/L = 1200). 6,13-bis(triisopropylsilylethynyl)pentacene (TIPS-PEN, Sigma–Andrich, Merck KGaA, Germany) and N,N′-bis-(2-ethylhexyl)−1,7-dicyanoperylene-3,4:9,10-bis(dicarboximide) derivative (ActivInk N140, Polyera Corporation, Flex Terra Corp, United States) were employed as organic semiconductors (OSCs). In particular, 0.5 wt.% solution using toluene (Sigma–Aldrich, Merck KGaA, Germany) was employed for preparing the TIPS-PEN based devices, while a 1 wt.% solution in 1,2 dichlorobenzene (Sigma–Aldrich, Merck KGaA, Germany) was used for the N1400-based transistors. Organic semiconductor deposition was performed in ambient conditions for all the fabricated devices. TIPS-PEN was deposited by drop casting the solution directly on the interdigitated structure, keeping the substrate at a constant temperature of 80 °C during the deposition, while N1400 was deposited by spin coating (60 s s at 1500 rpm). For both an annealing step (30 min at 80 °C) was carried out after the deposition.

*AFM Characterization*: AFM measurements were obtained by means of a SPM SOLVER PRO by NT-MDT in semi-contact mode using NT-MDT NSG01 tips.

*XRD Characterization*: XRD measurements were carried out at room temperature on a Bruker D8 Advance diffractometer using Cu K$\alpha$ radiation (40 kV, 40 mA) and a LYNXEYE XE-T detector operating in 1D high-resolution mode. Samples were placed on a UMC motorized stage, and the correct sample height was determined by means of a Z-scan. A Motorized Air Scatter Screen (MASS) was kept at a distance of 1 mm from the sample surface during data collection. XRD data were collected between 3 and 35° (2$\theta$) using Soller slits (2.5°) on both primary and secondary sides, a 0.01 mm divergence slit, and a step size of 0.02°.

## Acknowledgements

The authors kindly acknowledge CeSAR – University of Cagliari (Italy) for giving access to the XRD facility. G.C., P.C., S.L., and A.M. gratefully acknowledge the European Union for funding this activity under the project BioMeld (grant agreement No. 101070328). P.C. and A.M. acknowledge financial support from "Technologically Scalable 2D Materials and Extended Operando Measurement Methodologies for Advanced Device Fabrication" 2D-EMMA project – funded by European Union – Next Generation EU within the PRIN 2022 program (D.D. 104 – 02/02/2022 Ministero dell'Università e della Ricerca).

## Conflict of Interest

The authors declare no conflict of interest.

## Data Availability Statement

The data that support the findings of this study are available from the corresponding author upon reasonable request.

## Keywords

mechanical sensor, N1400, OFET, strain, tips-pentacene

Received: September 30, 2024
Revised: October 22, 2024
Published online: November 26, 2024

[1] W. Shi, Y. Guo, Y. Liu, *Adv. Mater.* **2020**, *32*, 1901493.
[2] K. Liu, B. Ouyang, X. Guo, Y. Guo, Y. Liu, *Npj Flex. Electron.* **2022**, *6*, 1.
[3] S. Park, M. Takakuwa, K. Fukuda, S. Lee, T. Yokota, T. Someya, *MRS Bull.* **2023**, *48*, 999.
[4] A. Spanu, T. Losi, A. Mascia, A. Bonfiglio, M. Caironi, P. Cosseddu, *Adv. Mater. Technol.* **2023**, *8*, 2200891.
[5] V. Pecunia, L. Petti, J. B. Andrews, R. Ollearo, G. H. Gelinck, B. Nasrollahi, J. M. Jailani, N. Li, J. H. Kim, T. N. Ng, H. Feng, Z. Chen, Y. Guo, L. Shen, E. Lhuillier, L. Kuo, V. K. Sangwan, M. C. Hersam, B. Fraboni, L. Basiricò, A. Ciavatti, H. Wu, G. Niu, J. Tang, G. Yang, D. Kim, D. Dremann, O. D. Jurchescu, D. Bederak, A. G. Shulga, et al., *Nano Futur* **2024**, *8*, 032001.
[6] Y. Yan, Y. Zhao, Y. Liu, *J. Polym. Sci.* **2022**, *60*, 311.
[7] Y. Xie, C. Ding, Q. Jin, L. Zheng, Y. Xu, H. Xiao, M. Cheng, Y. Zhang, G. Yang, M. Li, L. Li, M. Liu, *SmartMat* **2024**, *5*, e1261.
[8] Z. Shen, W. Huang, L. Li, H. Li, J. Huang, J. Cheng, Y. Fu, *Small* **2023**, *19*, 2302406.
[9] W. Tang, Y. Fu, Y. Huang, Y. Li, Y. Song, X. Xi, Y. Yu, Y. Su, F. Yan, X. Guo, *Npj Flex. Electron.* **2022**, *6*, 18.
[10] X. Jiang, C. Shi, Z. Wang, L. Huang, L. Chi, *Adv. Mater.* **2024**, *36*, 2308952.
[11] A. Mascia, A. Spanu, A. Bonfiglio, P. Cosseddu, *Sci. Rep.* **2023**, *13*, 16232.
[12] M. Concas, A. Mascia, S. Lai, A. Bonfiglio, P. Cosseddu, *Adv. Mater. Technol.* **2024**, 2400534.
[13] F. Wu, Y. Liu, J. Zhang, S. Duan, D. Ji, H. Yang, *Small Methods* **2021**, *5*, 2100676.
[14] P. Kubik, W. Waliszewski, A. Nosal, M. Tomczyk, A. Adamski, M. Gazicki-Lipman, P. W. M. Blom, T. Marszalek, W. Pisula, *Adv. Mater. Interfaces* **2022**, *9*, 2200206.
[15] S. Guo, Z. Wang, Y. Ma, J. Qi, S. Sun, L. Yuan, Y. Hu, Y. Huang, S. Wang, X. Chen, J. Li, L. Li, W. Hu, *ACS Appl. Mater. Interfaces* **2023**, *15*, 27010.
[16] S. Guo, X. Wang, J. Sun, Y. Tong, Q. Tang, Y. Liu, *IEEE Electron Device Lett.* **2023**, *44*, 1853.
[17] D. Skaf, T. C. Gomes, R. N. Hussein, G. Nagesh, M. J. Ahamed, T. B. Carmichael, S. Rondeau-Gagné, *ACS Appl. Polym. Mater.* **2024**, *6*, 4025.
[18] T. Sekitani, S. Iba, Y. Kato, T. Someya, *Jpn. J. Appl. Phys.* **2005**, *44*, 2841.
[19] T. Sekitani, Y. Kato, S. Iba, H. Shinaoka, T. Someya, T. Sakurai, S. Takagi, *Appl. Phys. Lett.* **2005**, *86*, 073511.
[20] V. Scenev, P. Cosseddu, A. Bonfiglio, I. Salzmann, N. Severin, M. Oehzelt, N. Koch, J. P. Rabe, *Org. Electron.* **2013**, *14*, 1323.
[21] P. Cosseddu, G. Tiddia, S. Milita, A. Bonfiglio, *Org. Electron.* **2013**, *14*, 206.
[22] D. J. Lipomi, *Adv. Mater.* **2016**, *28*, 4180.
[23] P. Cosseddu, S. Milita, A. Bonfiglio, *IEEE Electron Device Lett.* **2012**, *33*, 113.

[24] K. Fukuda, K. Hikichi, T. Sekine, Y. Takeda, T. Minamiki, D. Kumaki, S. Tokito, *Sci. Rep.* **2013**, *3*, 2048.
[25] H. Wang, Y. Tong, X. Zhao, Q. Tang, Y. Liu, *Org. Electron.* **2018**, *61*, 304.
[26] S. Lai, A. Garufi, F. Madeddu, G. Angius, A. Bonfiglio, P. Cosseddu, *IEEE Sens. J.* **2019**, *19*, 6020.
[27] T. Cramer, L. Travaglini, S. Lai, L. Patruno, S. De Miranda, A. Bonfiglio, P. Cosseddu, B. Fraboni, *Sci. Rep.* **2016**, *6*, 38203.
[28] S. Lai, I. Temiño, T. Cramer, F. G. Del Pozo, B. Fraboni, P. Cosseddu, A. Bonfiglio, M. Mas-Torrent, *Adv. Electron. Mater.* **2018**, *4*, 1700271.
[29] L. Ferlauto, F. Liscio, E. Orgiu, N. Masciocchi, A. Guagliardi, F. Biscarini, P. Samorì, S. Milita, *Adv. Funct. Mater.* **2014**, *24*, 5503.
[30] X. Xu, T. Xiao, X. Gu, X. Yang, S. V. Kershaw, N. Zhao, J. Xu, Q. Miao, *ACS Appl. Mater. Interfaces* **2015**, *7*, 28019.
[31] J. E. Anthony, J. S. Brooks, D. L. Eaton, S. R. Parkin, *J. Am. Chem. Soc.* **2001**, *123*, 9482.